The spectra of hydrogen and deuterium interpreted with an alternative fine structure constant compared to the CODATA recommended value.

Hans Peter Good
Sargans, Switzerland
e-mail: hp.good at catv.rol.ch

April 15, 2025

Abstract

A modified Dirac expression for the electron binding energy in hydrogen-like atoms is presented, which allows a direct and unambiguous comparison among different fine structure constants without bound-state QED theory. The least squares analysis of the parameters, describing the spectra of hydrogen and deuterium, is grounded on two sets of the most accurately measured energy separations. The optimal spectroscopic fine structure constant is experimentally found to be equal to 0.00 72 84(1), disagreeing with the determinations ultimately based on renormalized QED but being in good agreement with the number constant $2^{-6}\pi^{-\frac{2}{3}} \approx 0.00\ 72\ 84\ 28$. The present work compiles experimental values of the Lamb shift of S, P, and D states with n = 1, 2, and 3 derived from those measurements. Accurate predictions for hyperfine splitting intervals with n > 1 are given and compared with experimental values for n = 2.

Keywords: fine structure constant, bound-state QED, Dirac binding energy, hydrogen-like atoms, Lamb shift, hyperfine splitting.

Introduction

Currently, the fine structure constant $\alpha_{Codata} \approx 0.00\ 72\ 97\ 35$ is derived via a Dyson power series in powers of the fine structure constant α for the anomalous magnetic moment of the electron. The coefficients of this power series are not measurable and are calculated via many hundred complicated Feynman multiloop diagrams of quantum electrodynamics (free QED) that only a handful of theoretical physicists can master. Determinations of the fine structure constant by other means (quantum Hall effect, ac Josephson effect) also depend on QED and produce identical results that agree with each other with a precision of better than one part per 10^8 [1:p.20]. This is not surprising because various methods must produce the same result irrespective of the correctness of QED since they are based on the same theory. Unfavorably, extracting the fine structure constant from QED itself is not possible.[1] The spectrum of hydrogen, as the main

[1] Quotation from Kinoshita 1996, p. 25: As I have emphasized, QED (or its generalization, the standard model) is the fundamental theory which unifies all theories of low energy physics. In particular, all determinations of the fine structure constant α discussed in this review must lead to an identical result. This is irrespective of the fact that QED (or the standard model), which depends on external parameters such as e and m that cannot be generated from within the theory, is not yet close to the ultimate theory.

historical source of the value for the fine structure constant, no longer plays a role in the calculation of its value [2], and the spectrum is used solely to calculate the auxiliary Rydberg constant R_∞ of infinitely heavy mass, with the unit of energy (J) defined as $R_\infty \equiv \frac{1}{2}\alpha^2 m_e c^2$, acting by its definition as a universal scaling factor for all transitions and substituting for either the electron mass m_e or the fine structure constant α as needed.[3]

The author [2:p.42] derived the fine structure constant α_{geom} represented by the unit invariant number constant $\alpha_{geom} \equiv 2^{-6}\pi^{-\frac{2}{3}} \approx 0.00\,72\,843$ ($\alpha^{-1} \approx 137.28$). This idea does not require a formula for an observable quantity from which the fine structure constant is evaluated.

Model: an empirical modification to the Dirac equation

In the following, an algebraic scaling formula is presented that allows to decide, using the spectra of hydrogen (H) and deuterium (D), whether α_{Codata} or α_{geom} describes its spectrum better. In an arbitrary hydrogen-like atom, the electron binding energy $E(n, \ell, j)$ in the natural energy (J) unit $\{m_e c^2\}_{\text{Codata 2010}}$ shall be represented for the $S(\ell = 0)$, $P(\ell = 1)$, and $D(\ell = 2)$ states as

$$E(n, \ell, j) = E_D(n, j) \cdot \gamma \cdot \{1 + A + \delta_{\ell 0} B/n + \delta_{\ell 1}\delta_{k1} C/n + \delta_{\ell 1}\delta_{k2} D/n + \delta_{\ell 2}\delta_{k2} E/n + \delta_{\ell 2}\delta_{k3} F/n\} \qquad (1)$$

δ is the Kronecker delta function, and γ is a scaling factor of all levels that creates a fictitious Dirac particle with mass $\gamma\{m_e\}_{\text{Codata 2010}}$ moving in the field of a stationary point nucleus, and reducing the two-body problem to an equivalent one-body problem. This concept is not the correct treatment of the relativistic two-body quantum problem and is arbitrarily chosen as the starting point (gross structure, Δn ≠ 0) needing correction. The dimensionless, relativistic Dirac binding energy $E_D(n, j)$ for a fixed point nucleus Coulomb potential is analytically given by

$$E_D(n, j) = f(n, j) - 1$$

where [CODATA 2018, eq. 25; Kramida, eq. 3]

$$f(n, j) = \left[1 + \left(\frac{Z\alpha}{n - \delta}\right)^2\right]^{-\frac{1}{2}}$$

$$\delta = k - [k^2 - (Z\alpha)^2]^{\frac{1}{2}}$$

$$k = j + 1/2$$

Z is the nuclear integer-charge, n is a positive integer called the principal quantum number, $\ell = 0{,}1\ to\ n - 1$ is the orbital angular momentum, and $j = \ell \pm 1/2$ is the total angular momentum of the electron, which results from combining the orbital motion of the electron with its intrinsic angular momentum called spin. The Dirac binding energy fails to consider the nuclear mass and recoil and provides the same energy levels for each atom. Additionally, effects caused by the difference in the nuclear charge distribution are not included. In all the expressions, the Planck

---

[2] Quotation from Kramida 2010, p. 608: It is not easy to compare the experimental energy levels and transition frequencies of H, D, and T with the QED calculations because the latter are in fact adjusted to fit the experimental transition frequencies by adjusting the fundamental constants entering into the QED equations.

[3] Quotation from Kinoshita 1996, p. 6: In order to determine R [R_∞, note from the author] as accurately as in (7) [three parts per 10^{11}; note from the author], it is necessary to know the theoretical energy levels of the hydrogen atom to high precision. This requires determination of these levels including various radiative and recoil corrections using the full power of QED.

constant $\{h\}_{\text{Codata 2010}}$ is suppressed because it is solely used as a conversion factor to convert energy (J) to frequency (Hz). Formula (1) is a mathematical extension of the Dirac equation using the smallest number of model-independent parameters (perturbations) with a 1/n scaling law to describe experimental facts. The physical interpretation of the perturbations parameterized by the number set *B* to *F* is not part of this article.

Each hydrogenic atom has its own unique parameter set *A* to *F*, which must be experimentally determined. They are corrections to the scaled Dirac energy levels $E_D(n,j)\gamma$, neglecting the hyperfine structure ($\Delta F \neq 0$), and depend on the nucleus and the charge *Z*. Accounting for perturbations of levels with values of orbital angular momentum $\ell > 2$ is easily possible by analogy. With formula (1), a nucleus with one electron infinitely far away and no other electrons nearby has zero binding energy, so all bound state energy levels are negative. The ℓ dependent terms in formula (1) remove the degeneracy in ℓ and produce a splitting of levels with the same value of *j* but different values of ℓ, for example, between 2S1/2 and 2P1/2, which is convincingly proven to exist by WE Lamb and RC Retherford who reported a splitting of 1062(5) MHz [3]. For this reason, the splitting of levels ($\Delta\ell \neq 0$) was later called the Lamb shift and since then was theoretically explained by bound state QED, in contrast to ordinary QED for free leptons.[4]

The energy difference ΔE between two energy states is given by $\Delta E \equiv E(n_2,\ell_2,j_2) - E(n_1,\ell_1,j_1)$. The ionization energy of the ground state is $I \equiv \Delta E = E(n_2 \to \infty, 0, 1/2) - E(1,0,1/2)$ or $-E(1,0,1/2)$, which is the negative of the ground state energy and the largest energy for each atom. A common, accurate method of estimating absolute ionization energies is based on a fit of the modified Ritz formula. Using a Ritz series formula does not depend on theoretical calculations of the binding energy of any level and is an independent test of the validity of the fine structure constant (see note 'a' in Table 4 and Table 5).

According to formula (1), the transition 2S1/2–4S1/2 energy difference is

$$\Delta E = \left(E_{D(4,1/2)} - E_{D(2,1/2)}\right)\gamma + A\left(E_{D(4,1/2)} - E_{D(2,1/2)}\right)\gamma + B\left(\frac{E_{D(4,1/2)}}{4} - \frac{E_{D(2,1/2)}}{2}\right)\gamma = \Delta E^{meas}$$

and for the classic Lamb shift 2P1/2–2S1/2, which is difficult to measure because of the very short lifetime (natural line width 100 MHz) of the 2P1/2 state, the energy difference is

$$\Delta E = \left(E_{D(2,1/2)} - E_{D(2,1/2)}\right)\gamma + A\left(E_{D(2,1/2)} - E_{D(2,1/2)}\right)\gamma + B\frac{E_{D(2,1/2)}}{2}\gamma - C\frac{E_{D(2,1/2)}}{2}\gamma$$
$$= \frac{1}{2}(B - C)E_{D(2,1/2)}\gamma = \Delta E^{meas}$$

For each transition, analogous relations can be written to represent, in most cases, an overdetermined linear system of equations for the parameters *A, B, C, D, E,* and *F*, which has a least squares solution dependent on γ and α if the equations are linearly independent. The least squares solution best reproduces the input data or the results of the measurements via expression (1). The energy $E(n,\ell,j)$ calculated with the solutions of the normal equations via formula (1) is independent [5] of the scale factor γ and only depends on $Z\alpha$ and quantum numbers. This formalism allows, on the basis of a set of measured energy separations, a direct and unambiguous comparison among different fine structure constants without theory (bound-state QED), except

---

[4] Relation 15.3 in reference [2:p.184] is an incorrect ansatz because it does not take into account the Lamb shift. All results related to relation 15.3 must be reconsidered.

[5] This is because the scaling relations $A' = \frac{1-\gamma+A}{\gamma}$, $B' = \frac{B}{\gamma}$, $C' = \frac{C}{\gamma}$, $D' = \frac{D}{\gamma}$, $E' = \frac{E}{\gamma}$, $F' = \frac{F}{\gamma}$ apply.

the relativistic Dirac equation, in the analysis. Since formula (1) is based on the Dirac equation, the model is consistent with relativistic quantum mechanics.

Fine structure constant

In Table C, Kramida [4] tabulated the most accurately measured [6] fine structure intervals (differences between the corresponding energy levels) for hydrogen. Table 1 of this article is a copy of Kramida's Table C with two additional measurements at the end for the transitions 1S1/2–3S1/2 and 2S1/2–8D5/2. To derive the fine-structure energy levels listed in Table 1 from the available experimental data, purely theoretical corrections using α_{Codata} were necessary owing to the hyperfine splitting (hfs) of one or both fine-structure levels involved in the measured transition. Thus, most transitions listed in Table 1 cannot be considered purely experimental, and small systematic errors are most likely to exist in the input data (see Kramida 2010 section 4).

The reported intervals detailed in Table 1 were utilized to adjust the six parameters $A_{\_hyd}$ to $F_{\_hyd}$ by solving the linear system of equations. The measurements marked "not used" were not used to determine the best compromise values of $A_{\_hyd}$ to $F_{\_hyd}$, which only approximately satisfy all the measured intervals. In total, there are six degrees of freedom to fit 29 input values, that is, transition frequency measurements. The reliability of the observations was not included in the calculation because of unknown systematic uncertainties previously addressed.

The scaling factor has no influence on the energy values and can be arbitrarily set to one. Table 1 lists, for the 29 measurements considered, the calculated differences $Diff(\alpha) \equiv \Delta E^{meas} - \Delta E(\alpha)$ for $\alpha = \alpha_{Codata\,2010}$ and $\alpha = \alpha_{geom}$. The mean absolute deviation (MAD) of the 29 input values (results of the measurements) is 4.03 MHz for $\alpha_{Codata\,2010}$ and 0.82 MHz for α_{geom}. For deuterium, Kramida [4] displayed the most accurately measured fine structure intervals in Table G replicated in Table 2 of this article. To adjust the parameters $A_{\_deut}$ to $F_{\_deut}$, 19 linear equations in six unknowns were utilized, resulting in mean absolute deviations of 4.75 MHz for $\alpha_{Codata\,2010}$ and 0.80 MHz for α_{geom}. Minimizing the function $MAD(\alpha)$ yields the optimal fine structure constant α_{min} without knowing the scaling factor, that is, the Rydberg constant R_{atom}, meaning that the experimental values extracted are disentangled from the measurement of the absolute value of the Rydberg constant. The values obtained are displayed in Table 3, indicating that for both isotopes, the spectroscopic fine structure constant $\alpha_{spec} \equiv \alpha_{min} = 0.00\,72\,84(1)$ is very close to α_{geom} and strongly disagrees [7] with $\alpha_{Codata\,2010}$. The situation is shown graphically in Figure 1.

Historically, the optimal spectroscopic fine structure constant α_{spec} agrees with that found by Houston [5], who calculated a value of $\alpha \approx 0.00\,72\,85$ ($\alpha^2 \approx 5.307 \times 10^{-5}$) from purely spectroscopic measurements of the Rydberg constants for hydrogen and helium. Houston 1927

---

[6] This is mostly possible due to progress in the so-called Doppler-free two-photon spectroscopy, eliminating measurement errors due to the first order Doppler effect.

[7] Quotation from Kinoshita 1996, p. 25: If the complete consistency of α is not achieved in spite of further theoretical and experimental efforts, we may have to conclude that it is not interpretable within the framework of the known physics. Whether this leads to a breakdown of physics as we now know it, and possibly indicates the emergence of new physics, we are not able to say at present. One can only maintain that such a breakdown, if it occurs, cannot be attributed to the failure of QED at short distances. Indeed, not just QED, but also the standard model of the electroweak and strong interactions, or even the string theory, will be powerless to resolve the issue in such a case.

assumed in his evaluation that the relativity equation of Sommerfeld is applicable. In 1930, Millikan [6] noted that the experimental situation clearly favored, owing to his oil drop work, a value of $\alpha \approx 0.00\ 72\ 84$ ($\alpha^{-1} \approx 137.29$) that Birge [7] confirmed with the value $\alpha^{-1} = 137.31(5)$ in 1932 by the simultaneous evaluation of the electron charge and the Planck constant from several known functional relationships between these two constants. It would be interesting to look at the history of the measurements after Millikan to extract why the physics community settled down to the fine structure constant $\alpha \approx 0.00\ 72\ 97\ 35$, and today is aimlessly shifting the accuracy to ever higher decimal places.[8]

Figure 1: The mean absolute deviation (*MAD*) for hydrogen and deuterium as a function of the fine structure constant α.

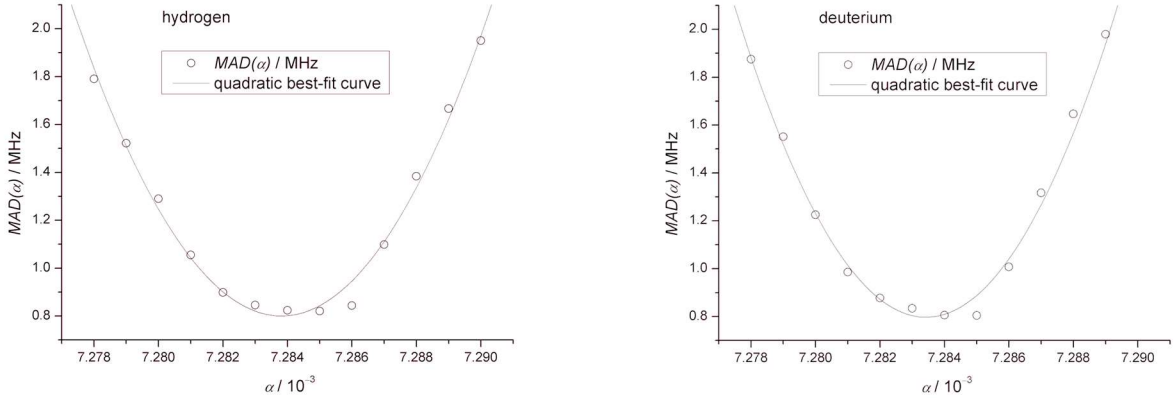

Kramida 2010 derived optimized energy levels from the measured fine structure intervals listed in Table 1 using a least-squares optimization (LOPT) code. The level optimization procedure involved several iterations via various interpolation and extrapolation procedures and the fitting of the Ritz series formulas for the nD5/2 and nS1/2 series. Table 4 is a copy of Kramida's Table 5 with 148 frequency intervals, which resulted from the semiempirical least-squares level optimization procedure. The absolute ionization energies tabulated by Kramida 2010 and NIST are additionally included in Table 4. The mean absolute deviations of the 148 high precision determinations (Ritz values) from the frequencies calculated via formula (1) are 3.67 MHz for $\alpha_{Codata\ 2010}$ and 0.78 MHz for α_{geom}. Ritz values do not depend on theoretical calculations of the binding energy of any level.

For deuterium, the measured fine-structure intervals from Table 2 were used to derive the energy levels using the LOPT code. Table 5 lists the Ritz values of 116 intervals resulting from the least squares level optimization procedure of Kramida, which is similar to that employed for hydrogen. In Table 5, the ionization energies tabulated by Kramida 2010 and NIST are also included. The mean absolute deviations of the 116 Ritz values from the frequencies calculated via formula (1) are 2.96 MHz for $\alpha_{Codata\ 2010}$ and 1.15 MHz for α_{geom}. All mean absolute deviations, which are mentioned in the text, are summarized in Table 6.

In all the cases, α_{geom} gives significantly smaller mean absolute deviations and describes, without further assumptions, the fine-structure energy levels of H and D more accurately by applying the

[8] Quotation from Kinoshita 1996, p. 25: Michelson's nightmare of aimlessly pushing back the decimal points might become a reality some day. What I have tried to show in this review is that the sterility one might expect is not yet present; on the contrary…….

simple expression (1). In summary, there is convincing spectroscopic experimental evidence that the fine structure constant α based on renormalized QED determinations should be discarded.

Table 6: Summary of the mean absolute deviations (*MAD*).

intervals		# of intervals	*MAD* (MHz) α_{geom}	*MAD* (MHz) $\alpha_{Codata\ 2010}$
Table 1	H	29	0.82	4.03
Table 4	H	148	0.78	3.67
Table 2	D	19	0.80	4.75
Table 5	D	116	1.15	2.96

Lamb shift

Without knowing the exact scale factor γ and the fine structure constant, Lamb shifts cannot be extracted from the spectra. First, a clear definition is vital to avoid different interpretations of the term Lamb shift. Using formula (1), the definition for the Lamb shift $\mathcal{L}(nS1/2)$ is as follows:

$$\mathcal{L}(nS1/2) \equiv \mathcal{L}(n,0,1/2) \equiv E_D(n,1/2)\cdot\gamma\cdot\{A+B/n\} = E_D(n,1/2)\cdot\gamma_{zero}\cdot B/n \qquad (2)$$

which can easily be generalized to other Lamb shifts $\mathcal{L}(n,\ell,j)$. The choice of γ defines the values of the Lamb shifts, which are to be understood as effects in addition to what can be obtained from the scaled Dirac equation. In the literature, the reference point is not unique due to different corrections applied and, in most cases, is even undefined. One possibility for an "experimental" reference point is to choose the scaling factor such that for $\gamma = \gamma_{zero}$ the parameter A is zero, which implicitly defines γ_{zero} by $A(\gamma_{zero}) = 0$ or explicitly [9] by $\gamma_{zero} \equiv 1 + A(\gamma = 1)$. The corrections that affect all states are ascribed to the scaling factor γ_{zero} and the parameters *B* to *F*, which may be called dimensionless Lamb shift constants, include all the corrections that cannot be described by γ_{zero}. The scaling factor γ_{zero} completely relies on an experimental input, to wit, Table 1 or Table 2. The adjusted dimensionless parameters *B* to *F* and the experimentally determined absolute Lamb shifts for *n = 1, 2,* and *3* are detailed for $\alpha = \alpha_{Codata\ 2010}$, $\alpha = \alpha_{geom}$, and $\gamma = \gamma_{zero}(\alpha)$ in Table 3. Purely experimental data for γ_{zero} and the Lamb shift $\mathcal{L}(n,\ell,j)$ are obtained using $\alpha = \alpha_{min}$, which is not listed in Table 3 because of $\alpha_{min} \approx \alpha_{geom}$. In this case, only $\{m_e c^2/h\}_{\text{Codata 2010}}$ is involved in evaluating the experimental data for the parameters from the input data.

To clarify the significance of the theoretical corrections to the experimental data mentioned in the text, only the two gross structure transitions 1S1/2–2S1/2 and 2S1/2–8S1/2 from Table 1 (Kramida 2010, column largest theoretical correction) were fitted to the two data points, from which exact ($MAD(\alpha_{geom})$=0) values for [γ_{zero}] and the parameter [*B*], scaling the Lamb shifts of the nS1/2 levels in terms of the principal quantum number n, can be extracted. The results are displayed in brackets in Table 3, which give 2 466 061 413.1859 MHz for the 1S1/2–2S1/2 interval and 770 649 350.012 MHz for the 2S1/2–8S1/2 interval. The measured values [10] are

[9] The explicit expression follows from the scaling relation $A' = 0 = \frac{1-\gamma_{zero}+A(\gamma=1)}{\gamma_{zero}}$.

[10] The exact measurements are not obtained because the numbers in Table 3 are rounded to 12 decimal places.

marked with an asterisk (*) in Table 1. The fitted parameter [B] is an accurate experimental value allowing direct comparison for $\alpha = \alpha_{geom}$ with nS1/2 Lamb shift calculations, which are currently performed within the framework of bound state QED.

Finite mass

For a nucleus of finite mass M, nuclear motion is accounted for nonrelativistically by replacing the electron mass m_e with the reduced mass, which multiplies all energy levels by the reduced mass correction factor $\gamma_{red\ mass} \equiv \left(1 + \frac{m_e}{M}\right)^{-1}$. These factors are tabulated for hydrogen and deuterium in Table 3 using CODATA 2010 values for the electron–nuclear mass ratios on the basis of high precision Penning trap mass spectrometry. A comparison of the factors $\gamma_{red\ mass\ Codata\ 2010}$ for both isotopes with the experimental scaling factors $\gamma_{zero}(\alpha_{Codata\ 2010})$ reveals that they are nearly equal (Table 3).

Interestingly, if the experimental scaling factors $\gamma_{zero}(\alpha_{geom})$ are divided by the correction factor

$$\gamma_{corr} \equiv \left(\frac{\alpha_{Codata\ 2010}}{\alpha_{geom}}\right)^2 \approx 1.003\ 591\ 800 \qquad (3)$$

the results are 0.999 455 690 for H compared to the CODATA 2010 reduced mass factor of 0.999 455 679, and 0.999 727 643 for D compared to 0.999 727 631, which means that the simple reduced mass correction factors for both isotopes are derived for α_{geom} very accurately from essentially experimental spectroscopic data, implying a reduction of the relativistic two body problem to an equivalent one body equation in terms of a single effective mass. The deviations relative to the tabulated reduced mass factors $\gamma_{red\ mass\ Codata\ 2010}$ are 1.0 parts per 10^8 for H and 1.2 parts per 10^8 for D.

The close agreement

$$\gamma_{zero}(atom) \approx \gamma_{red\ mass}(atom) \times \gamma_{corr} \qquad (4)$$

is quite remarkable, since the concept of reduced mass has no theoretical basis in relativistic quantum mechanics, and the assumption that the nucleus behaves inertly and plays no role other than its mass is an idea of the classic Bohr model. The factor γ_{corr} might be interpreted as a correction of the spectroscopic electron mass $\{m_e\}_{\text{Codata 2010}}$ deduced by CODATA from experimental data through a least squares adjustment with the fine structure constant $\alpha_{Codata\ 2010}$ determined by other independent measurements (nonspectroscopic), assuming for the energy level the expression [CODATA 2010, equ. 22]

$$E(n,\ell,j) = -\frac{Z^2 R_\infty}{n^2}\{1 + \delta(n,\ell,j)\} \equiv -\frac{Z^2 R_\infty}{n^2} F_{n\ell j}^{rel}$$

where $\delta(n,\ell,j)$ is a dimensionless theoretical correction factor, small compared with one, that contains the details of the bound-state QED apparatus of each energy level, including the effect of the finite size of the nucleus as a function of the rms charge radius. Only the Rydberg constant R_∞ is an adjusted constant in the numerical evaluation carried out by CODATA. The method mentioned above consists of comparing measured transitions (primarily the 1S–2S frequency in H and the H–D isotope shift of the 1S–2S frequency) with intervals calculated from a complex theoretical equation for each energy level scaled with R_∞, which indirectly assigns, using α_{Codata},

a fitted value to the absolute electron mass $\{m_e\}_{\text{Codata}}$ that can by no means be directly compared (i.e., without a theoretical contribution) to the artifact SI standard kilogram.

There should be some skepticism regarding the strong connection between reduced mass factors calculated through formula (4) and those using mass spectrometry. Could the close agreement be a consequence of Codata already accounting for the reduced mass factor when computing the electron mass $\{m_e\}_{\text{Codata}}$ as previously described?

Tritium

Since tritium (T) is radioactive and difficult to handle, there is little information about its spectrum from which a reliable parameter set can be obtained. The Lamb shift parameters *B* to *F* of hydrogen and deuterium are similar in value, which suggests that the most accurate known Lamb shift parameters *B* to *F* of hydrogen could be used as a first approximation for tritium. The most accurate measured values of four fine structure transitions arranged by Kramida [4] in Table K are listed in Table 7 and compared with the values calculated via formula (1), using $\alpha = \alpha_{geom}$, $A = 0$, the parameters $B_{\_hyd}$ to $F_{\_hyd}$ of hydrogen (Table 3), and $\gamma = \gamma_{red\ mass}\,(T) \times \gamma_{corr}$.

Table 7: The most accurate measured fine structure transitions of tritium compared with calculated values via formula (1).

Tritium Fine structure transition	ΔE_{exp} (MHz) (mean meas. freq.)	Unc. (MHz) (exp.)	ΔE_{calc} (MHz)	$\Delta E_{exp\,-\,calc}$ (MHz)
2P3/2–3D5/2	456 841 568.8	1.6	456 841 565.6	3.2
2P1/2–3D3/2	456 851 457.2	1.3	456 851 461.5	−4.3
2S1/2–3P3/2	456 850 405.8	1.4	456 850 405.0	0.8
2S1/2–3P1/2	456 847 153.8	1.6	456 847 153.7	0.1

Hyperfine splitting

Formula (1) considers the Lamb shift as a perturbation to the scaled Dirac energy levels $E_D(n,j)\gamma$. In the following, the hyperfine splitting manifested as a small splitting of the fine-structure energy levels is regarded, analogous to the Lamb shift, as a perturbation to $E(n,\ell,j)$ of the form

$$E(n,\ell,j,F) = E(n,\ell,j)\{1 - Q(\ell,j,I,F)\cdot Z\cdot \tilde{B}/n\} \tag{5}$$

The number *I* is the spin of the nucleus, and *F* is the total angular momentum for the whole atom with possible values of $j+I,\ j+I-1,\ldots,|j-I|$. Formula (5) can be deduced from the rephrased equations 5 and 6 (without off-diagonal terms) given by Kramida 2010 by setting

$$\frac{Z^2 R_\infty}{n^2} F_{n\ell j}^{rel} \equiv -E(n,\ell,j)$$

$$\frac{[F(F+1) - I(I+1) - j(j+1)]}{j(j+1)(2\ell+1)I} \equiv Q$$

$$\alpha^2 \frac{\mu_{nucl}}{\mu_B} \equiv \tilde{B}$$

The minus sign in relation (5) ensures that the energy of the F level is lifted and that of F-1 is lowered. From formula (5), the hfs interval between two adjacent levels in a hyperfine multiplet can be written as

$$(\Delta E)^{hfs}_{n\ell j} = E(n,\ell,j,F) - E(n,\ell,j,F-1) = -E(n,\ell,j)\cdot\frac{2F}{j(j+1)(2\ell+1)I}\cdot Z\cdot\tilde{B}/n \qquad (6)$$

where Lamb shifts of energy levels are taken into account. Because the relativistic Dirac theory naturally implies that the electron's magnetic dipole moment is exactly $\mu_e = \mu_B$, the ratio $\frac{\mu_e}{\mu_B}$ in equation (6) given by Kramida 2010 was set to one. For simplicity requirements on the approximating function, the reduced mass prefactor $\gamma_{red\ mass}{}^3$ has been omitted, assuming that a correction in the form of an overall reduced mass factor is adequate. These assumptions make relation (6) compatible with the uncorrected expression (22.13) of Bethe and Salpeter [10], and equation (41) of Grifffiths [11] with g_e = 2.

The value of $\frac{\mu_{nucl}}{\mu_B}$ is not directly accessible experimentally, but it can be traced back to maser experiments by Winkler and coworkers, who determined the bound particle ratio of the magnetic moments of the nucleus and electron $\frac{\mu_{nucl}(atom)}{\mu_e(atom)}$, implying that the bound electron moment in Bohr magnetons $\frac{\mu_e(atom)}{\mu_B}$ must also be known. This ratio can be approximated by $\frac{\mu_e(geonium)}{\mu_B} \equiv 1 + a_e$, where a_e [Codata 2010] is the very accurately measured electron magnetic moment anomaly.[11] Replacing the fine structure constant α by α_{geom} implies that, in addition to 1+a_e, the multiplying factor γ_{corr} must be taken into account, since the electron mass is given by $\gamma_{corr}\{m_e\}_{Codata}$. Combining all this gives

$$\tilde{B} \equiv \alpha^2\frac{\mu_{nucl}}{\mu_B} = \alpha^2\cdot\frac{\mu_{nucl}}{\mu_e}\cdot\frac{\mu_e}{\mu_B} \approx \alpha^2\cdot\frac{\mu_{nucl}}{\mu_e}\cdot(1+a_e) \approx \alpha_{geom}{}^2\cdot\frac{\mu_{nucl}}{\mu_e}\cdot(1+a_e)\cdot\gamma_{corr} \qquad (7)$$

Table 8 lists the hyperfine splittings of hydrogen and deuterium, which were calculated via relation (6) and hypothesis (7). The scaling factor γ_{zero} ([γ_{zero}] for H) and the parameter B ([B] for H) used to compute $E(n,\ell,j)$ correspond to the values listed in Table 3. All four factors ultimately leading to relation (7) are essentially experimental in nature when α_{geom} is replaced by α_{spec}.

Table 8: Hyperfine splittings of hydrogen and deuterium calculated via relation (6) and hypothesis (7).

atom			$\frac{\mu_{nucl}(atom)}{\mu_e(atom)}10^3$ (meas.)		$(\Delta E)^{hfs}_{1S1/2}$ (MHz)			$\Delta E^{exp}/\Delta E^{calc}$
Z	I	F			(6) and (7)	experiment		(correction)
^{1}H 1	1/2	1	1.519 270 336	[12a]	1420.401	1420.406	[4]	1.000 003
^{2}H 1	1	3/2	0.466 434 539	[12b]	327.149	327.384	[4]	1.000 718

A comparison of the theoretical results with the experimental values reveals a remarkable agreement (or coincidence?) with a precision of 3 parts per 10^6 for hydrogen [12], and reflects an

---

[11] The metastable pseudo-atom geonium is an individual electron that is permanently confined in an ultrahigh vacuum Penning trap at 4K. The trap employs a homogeneous magnetic field and a weak electric quadrupole field.

[12] The pure QED estimate is 1420.451 99(14) MHz [1:p.5]. Due to "lack of knowledge" about the structure of the proton, the necessary nuclear correction terms cannot or only vaguely be calculated, and the high measurement accuracy of the hyperfine splitting of atomic hydrogen is not used today for the determination of natural constants.

unclear discrepancy with a substantial correction factor for deuterium. This might be because the ratio of the magnetic moment of the deuteron to the magnetic moment of the electron in the 1S state of deuterium has never been published. This magnetic ratio should be reevaluated.

Scaling law for hfs intervals

Owing to the lack of knowledge on the number of multiplying factors that control hypothesis (7), the dimensionless parameter $\tilde{B}$, which is responsible for splitting, is difficult to calculate. However, the existence of high-precision experimental data on the 1S hfs splitting makes it possible to derive an empirical, simple scaling law for other hfs intervals, if the dimensionless parameter $\tilde{B}$ is the same for all levels. For hydrogen, the scaling law from the ground-state hyperfine splitting is then

$$(\Delta E)^{hfs}_{n\ell j}(F-1;F) = (\Delta E)^{hfs}_{1S1/2}(0;1)\cdot\frac{E(n,\ell,j)}{E(1,0,1/2)}\cdot\frac{F}{j(j+1)(2\ell+1)}\cdot\frac{3}{4}\cdot\frac{1}{n} \qquad (8)$$

For the scaling law from the ground-state hyperfine splitting of deuterium, the factor 3/4 in formula (8) must be replaced by 1/2. In Table 9, theoretical predictions via the scaling relation (8) are given and compared with experimental results for 2S1/2 states. The alignment between theory and experimental data is striking for both isotopes, featuring a consistent relative deviation of 30 ppm that does not vary with the nucleus. Unfortunately, besides the 2P1/2 hfs splitting in hydrogen of 59.22(14) MHz [Kramida 2010, Table A], no reliable experimental data are available for other excited states. In Kramida's work, one can find theoretical values derived by different authors employing QED with α_{Codata}, enabling a comparison with the calculations from expression (8). The predictions generated through the scaling relation (8) may be employed to iteratively calculate experimental corrections for the measured quantities (Table 1, Table 2).

Conclusion

There is no independent approach to determining the fine structure constant from the energy levels of hydrogen or deuterium. The energy intervals that were measured are utilized to calculate the mass of the electron, employing a fine structure constant that is not derived from spectroscopic evaluations. This study proposes a method to experimentally ascertain a spectroscopic fine structure constant α_{spec} that relies solely on the relativistic Dirac equation, free from other theoretical frameworks {$\gamma_{red\ mass}$(classical physics); α_{Codata}(QED); α_{geom}}. It's remarkable that the experimental spectroscopic fine structure constant closely matches the number constant $2^{-6}\pi^{-\frac{2}{3}}$, though this could be a mere coincidence.

The lowest term $\frac{\alpha}{2\pi}$ in the development of a_e was first derived by Julian Schwinger. It involves a single virtual exchange of a photon with the electron and is called one-loop correction or Schwinger correction. The relative deviation to the measurement is ≈ 0.152 % if only the one-loop correction $\frac{\alpha_{Codata}}{2\pi}$is taken into account. Although the Schwinger term $\frac{\alpha_{Codata}}{2\pi}$ already accounts for more than 99.8% of the total correction, only higher terms of the development, which reflect interaction processes with much less likelihood, significantly reduce the deviation from the measurement. Remarkably, the deviation from the measured value is approximately five times smaller (≈ 0.028 %) if α_{geom} is used in the one-loop term [2:p.45].

Interestingly, the model accurately reproduces the hyperfine splitting of hydrogen in its ground state with a precision of three parts per million, surpassing the results obtained through pure QED calculations. Furthermore, a basic scaling law enables the computation of hyperfine splittings solely from experimental data, achieving a relative deviation of 30 ppm for 2S1/2 states. Additionally, the determined absolute ionization energies for both isotopes fall within the error margins of the experimental Ritz series limits.

References

[1] The fine structure constant.
Toichiro Kinoshita Rep Prog Phys **59** 1459 (1996)

[2] On the Origin of Natural Constants.
Hans Peter Good, De Gruyter Berlin (2018)

[3] Fine Structure of the Hydrogen Atom. Part II
W E Lamb and R C Retherford Phys Rev **81**, 222 (1951)

[4] A critical compilation of experimental data on spectral lines and energy levels of hydrogen, deuterium, and tritium.
A E Kramida Atomic Data and Nuclear Data Tables **96** 586 (2010)

[5] A spectroscopic Determination of e/m.
W V Houston Phys Rev **30** 608 (1927), p. 613

[6] The most probable 1930 values of the electron and related constants.
R A Millikan Phys Rev **35** 1231 (1930), p. 1235

[7] Probable Values of e, h, e/m, and α.
R T Birge Phys Rev **40** 228 (1932)

[8] CODATA 2018, Table X

[9] Measurement of the 2S1/2–8D5/2 transition in hydrogen.
A D Brandt et al Phys Rev Lett **128** 023001 (2022)

[10] Quantum Mechanics of One- and Two-Electron Atoms.
H A Bethe, E E Salpeter, Springer-Verlag Berlin (1957), p. 110

[11] Hyperfine splitting in the ground state of hydrogen.
D J Griffiths Am J Phys **50** 698 (1982), p. 701

[12] CODATA 1998
a) Table XIV.B.1, B9 : Winkler et al Phys Rev A **5** 83 (1972)
b) Table XIV.B.1, B10 : Phillips et al (1984), private communication, unpublished result

Table 1: The best available measurements of fine-structure intervals in *hydrogen* [4].

interval		Measured value (MHz)	Unc. (MHz)	Diff (MHz)	
				α_{geom}	α_{Codata}
1S1/2–2S1/2	*	2466061413.187074	0.000034	−0.1	2.1
2P1/2–2S1/2		1057.847	0.09	−1.0	−2.3
2P1/2–2P3/2		10969.13	0.1	−0.1	−0.1
2S1/2–2P3/2		9911.201	0.012	0.8	2.1
2P1/2–3D3/2	not used	456685852.8	1.7		
2S1/2–3P1/2		456681549.9	0.3	−1.5	−5.1
2S1/2–3P3/2		456684800.1	0.3	−1.5	−5.0
3P1/2–3D3/2	not used	456675968.3	3.4		
2S1/2–4P1/2		616520017.568	0.015	−0.3	−3.0
2S1/2–4S1/2		616520150.636	0.01	0.4	−2.4
2S1/2–4P3/2		616521388.672	0.01	−0.3	−3.0
2S1/2–4D5/2		616521843.441	0.024	1.3	−9.6
2S1/2–6S1/2		730690017.097	0.021	0.2	−0.1
2S1/2–6D5/2		730690518.592	0.011	0.4	−2.3
2S1/2–8S1/2	*	770649350.012	0.09	0.3	1.5
2S1/2–8D3/2		770649504.45	0.08	0.0	0.4
2S1/2–8D5/2		770649561.584	0.06	0.3	0.5
2S1/2–10D5/2		789144886.411	0.039	0.2	1.7
2S1/2–12D3/2		799191710.473	0.09	0.1	2.4
2S1/2–12D5/2		799191727.404	0.07	0.2	2.4
3P1/2–3S1/2		314.818	0.048	1.1	0.7
3P1/2–3D3/2	not used	3244.9	3.1		
3S1/2–3P3/2	not used	2933.5	1.2		
3S1/2–3D3/2		2929.9	0.8	−3.8	−18.9
3S1/2–3D5/2		4013.155	0.048	2.6	−16.5
3D3/2–3P3/2		5.5	0.9	2.7	18.3
3D3/2–3D5/2	not used	1083	0.29		
3P3/2–3D5/2	not used	1078	1.1		
4P1/2–4S1/2		133.2	0.6	0.8	0.7
4P1/2–4P3/2		1370.85	0.22	−0.3	−0.3
4P1/2–4D3/2		1371.1	1.2	1.1	−5.5
4S1/2–4D3/2	not used	1235	2.1		
4S1/2–4P3/2		1237.79	0.29	−1.0	−0.8
4S1/2–4D5/2		1693	0.4	1.0	−7.0
4D3/2–4F5/2	not used	456.8	1.6		
4D3/2–4D5/2	not used	458	2.2		
4P3/2–4D5/2	not used	455.7	1.6		
4D5/2–4F7/2	not used	227.96	0.41		
5P1/2–5S1/2	not used	64.6	5		
5P1/2–5D3/2	not used	704	7		
5S1/2–5P3/2	not used	622	10		
5P3/2–5D5/2	not used	232.2	2.9		
5D5/2–5F7/2	not used	117	1.5		
1S1/2–3S1/2	[8]	2922743278.678	0.013	0.2	−1.5
2S1/2–8D5/2	[9]	770649561.5709	0.02	0.3	0.5

Table 2: The best available measurements of fine-structure intervals in *deuterium* [4].

interval		Measured value (MHz)	Unc. (MHz)	Diff (MHz)	
				α_{geom}	α_{Codata}
1S1/2–2S1/2		2466732407.52171	0.00015	0.1	0.5
2P1/2–2S1/2		1059.28	0.06	−0.7	−1.9
2S1/2–2P3/2		9912.61	0.3	−0.1	1.5
2P1/2–3D3/2		456810113.8	0.19	−6.0	−26.7
2S1/2–3P1/2		456805811.7	0.3	−0.7	−4.4
2S1/2–3P3/2		456809062.6	0.3	−0.9	−4.6
2P3/2–3S1/2	not used	456796251	30		
2P3/2–3D5/2		456800225.9	1.6	1.5	−23.4
2P1/2–4D3/2	not used	616690180	40		
2S1/2–4P1/2		616687769.99	0.19	−0.6	−3.5
2S1/2–4S1/2		616687903.573	0.02	0.5	−2.6
2S1/2–4P3/2		616689141.73	0.17	−0.4	−3.3
2S1/2–4D5/2		616689596.72	0.4	1.6	−9.5
2P3/2–4D5/2	not used	616679760	50		
2P1/2–5D3/2	not used	690691810	50		
2P3/2–5D5/2	not used	61681100	70		
2P1/2–6D3/2	not used	730890320	60		
2P3/2–6D5/2	not used	730879480	80		
2P1/2–7D3/2	not used	755128600	60		
2P3/2–7D5/2	not used	755117710	50		
2P1/2–8D3/2	not used	770860360	210		
2S1/2–8S1/2		770859041.246	0.07	0.2	1.1
2S1/2–8D3/2		770859195.702	0.006	0.0	0.1
2S1/2–8D5/2		770859252.850	0.06	0.4	0.2
2P3/2–8D5/2	not used	770849570	210		
2P1/2–9D3/2	not used	781645760	300		
2P3/2–9D5/2	not used	781634790	300		
2S1/2–10D5/2		789359610.238	0.038	0.2	1.4
2S1/2–12D3/2		799409168.038	0.09	0.0	2.0
2S1/2–12D5/2		799409184.967	0.07	0.1	2.1
3P1/2–3S1/2		315.3	0.4	1.2	0.9
3P1/2–3P3/2	not used	3250.7	1		
3S1/2–3P3/2	not used	2934.5	5		
3D3/2–3P3/2	not used	5	5		
4P1/2–4S1/2	not used	133	5		
4P1/2–4P3/2		1371.8	0.3	0.2	0.3

Table 3: The adjusted dimensionless parameters *A* to *F* and the absolute Lamb shifts for *n* = 1, 2, and 3.

isotope		*hydrogen*		*deuterium*	
Experimental input		Table 1		Table 2	
Number of input values		29		19	
α_{min}		≈ 0.00 72 839 [13]		≈ 0.00 72 833	
		$\alpha_{Codata\ 2010}$ (≈ 0.00 72 974)	α_{geom} (≈ 0.00 72 843)	$\alpha_{Codata\ 2010}$	α_{geom}
mean abs. dev.	(MHz)	4.03	0.82	4.75	0.80
γ_{zero}		0.999 455 610 362	1.003 045 534 235	0.999 727 563 649	1.003 318 464 318
$[\gamma_{zero}]$			[1.003 045 534 890]		
$\gamma_{red\ mass\_Codata\ 2010}$		0.999 455 679(1)		0.999 727 631(1)	
γ_{zero} / γ_{corr}			0.999 455 690		0.999 727 643
A all levels	(ppm)	0	0	0	0
B (nS1/2)		−2.411 846	−2.441 530	−2.419 799	−2.450 077
$[B]$			[−2.442 137]		
C (nP1/2)		0.167 457	0.134 688	0.161 442	0.128 073
D (nP3/2)		0.105 245	−0.022 870	0.098 994	−0.030 347
E (nD3/2)		0.148 730	0.022 573	0.217 980	0.049 010
F (nD5/2)	(ppm)	0.141 163	−0.021 527	0.189 677	−0.015 156
$\mathcal{L}(1S1/2)$	(MHz)	7930.4	8028.0	7958.7	8058.3
$\mathcal{L}(2S1/2)$		991.3	1003.5	994.8	1007.3
$\mathcal{L}(2P1/2)$		−68.8	−55.4	−66.4	−52.7
$\mathcal{L}(2P3/2)$		−43.3	9.4	−40.7	12.5
$\mathcal{L}(3S1/2)$		293.7	297.3	294.8	298.5
$\mathcal{L}(3P1/2)$		−20.4	−16.4	−19.7	−15.6
$\mathcal{L}(3P3/2)$		−12.8	2.8	−12.1	3.7
$\mathcal{L}(3D3/2)$		0.0	0.0	0.0	0.0
$\mathcal{L}(3D5/2)$	(MHz)	0.0	0.0	0.0	0.0

Notes:

The value α_{min} is the result of minimizing the mean absolute deviation (*MAD*) based on Table 1 or Table 2 using formula (1) and the solutions of the linear system of equations. The minima were determined by quadratic regression of 21 values of the discretized function *MAD(α;Table 1)* or *MAD(α;Table 2)* with α = [0.0072800, 0.0072900] and $\Delta\alpha$ = 0.0000005.

The gray-shaded fields present the adjusted dimensionless parameters in formula (1) to compute the binding energy $E(n, \ell, j)$ for α_{geom}. All numbers are rounded to 12 decimal places.

For the classic Lamb shift 2P1/2–2S1/2 of hydrogen the energy difference $E(2,1,1/2) - E(2,0,1/2)$ is 1058.86 MHz using $\{m_e c^2/h\}_{\text{Codata 2010}}$.

[13] The five pure S-state transitions, highlighted in bold in Table 1, yield α_{min} = 0.00 72 850(1) with $MAD(\alpha_{min})$ ≈ 0.042 MHz.

Table 4: Frequencies of fine-structure transitions in *hydrogen* derived from the level-optimization procedure [Kramida 2010, Table 5].

interval	ΔE_{Ritz} (MHz) (Ritz values)	Unc. (MHz)	$\Delta E_{Ritz} - \Delta E_{calc}$ (MHz) α_{geom}	α_{Codata}
Ionization [a]	**3288086856.8**	**0.7**	**−0.5**	**5.8**
Ionization [b]	3288086857.128	0.003	−0.1	6.1
1S1/2–2P1/2	2466060355.339	0.009	0.9	4.4
1S1/2–2S1/2	2466061413.18707	0.00003	−0.1	2.1
1S1/2–2P3/2	2466071324.389	0.012	0.7	4.2
1S1/2–3P1/2	2922742963.15	0.21	−1.6	−2.9
1S1/2–3S1/2	2922743277.97	0.22	−0.5	−2.2
1S1/2–3P3/2	2922746213.24	0.21	−1.7	−2.9
1S1/2–4P1/2	3082581430.756	0.015	−0.4	−0.8
1S1/2–4S1/2	3082581563.823	0.01	0.3	−0.3
1S1/2–4P3/2	3082582801.858	0.01	−0.5	−0.9
1S1/2–5P1/2	3156563616.6	1.1	0.0	0.9
1S1/2–5S1/2	3156563684.8	1.1	0.4	1.3
1S1/2–5P3/2	3156564318.6	1.1	−0.1	0.9
1S1/2–5D5/2	3156564549.7	0.7	−1.0	−4.2
1S1/2–6P1/2	3196751390.79	0.3	−0.2	1.8
1S1/2–6S1/2	3196751430.284	0.021	0.1	2.0
1S1/2–6P3/2	3196751797.05	0.03	−0.2	1.8
1S1/2–7P1/2	3220983314.5	1.2	−0.2	2.7
1S1/2–7S1/2	3220983339.4	1.2	0.0	2.8
1S1/2–7P3/2	3220983570.4	1.2	−0.2	2.7
1S1/2–7D5/2	3220983655.4	0.7	0.3	1.6
1S1/2–8P1/2	3236710746.525	0.018	0.0	3.5
1S1/2–8S1/2	3236710763.199	0.009	0.1	3.6
1S1/2–8P3/2	3236710917.916	0.019	0.0	3.5
1S1/2–9P1/2	3247493411.9	1.2	0.2	4.1
1S1/2–9S1/2	3247493423.6	1.2	0.2	4.2
1S1/2–9P3/2	3247493532.3	1.2	0.2	4.1
1S1/2–9D5/2	3247493572	0.7	0.1	3.3
1S1/2–10P1/2	3255206183.1	1.2	0.3	4.7
1S1/2–10S1/2	3255206191.6	1.2	0.4	4.7
1S1/2–10P3/2	3255206270.8	1.2	0.3	4.6
1S1/2–11P1/2	3260912757.7	1.2	0.3	4.9
1S1/2–11S1/2	3260912764.1	1.2	0.4	5.0
1S1/2–11P3/2	3260912823.6	1.2	0.3	4.9
1S1/2–11D5/2	3260912845.1	0.7	0.0	4.2
1S1/2–12P1/2	3265253073.3	1.2	0.3	5.1
1S1/2–12S1/2	3265253078.2	1.2	0.3	5.1
1S1/2–12P3/2	3265253124	1.2	0.2	5.1
2P1/2–2S1/2	1057.848	0.09	−1.0	−2.3
2P1/2–2P3/2	10969.05	0.015	−0.2	−0.2
2P1/2–3S1/2	456682922.63	0.22	−1.4	−6.6

Table 4: (continued)

interval	ΔE_{Ritz} (MHz) (Ritz values)	Unc. (MHz)	$\Delta E_{Ritz} - \Delta E_{calc}$ (MHz) α_{geom}	α_{Codata}
2P1/2–3D3/2	456685852.6	0.6	−5.0	−25.5
2P1/2–4S1/2	616521208.484	0.013	−0.6	−4.7
2P1/2–4D3/2	616522444.5	0.23	−2.2	−12.7
2P1/2–5S1/2	690503329.4	1.1	−0.5	−3.2
2P1/2–5D3/2	690503960.5	0.7	−3.1	−9.0
2P1/2–6S1/2	730691074.945	0.023	−0.8	−2.4
2P1/2–6D3/2	730691441.05	0.04	−1.4	−4.9
2P1/2–7S1/2	754922984.1	1.2	−0.9	−1.5
2P1/2–7D3/2	754923214.8	0.7	−1.1	−3.0
2P1/2–8S1/2	770650407.86	0.012	−0.8	−0.8
2P1/2–8D3/2	770650562.298	0.012	−1.0	−1.9
2P1/2–9S1/2	781433068.3	1.2	−0.6	−0.2
2P1/2–9D3/2	781433176.5	0.7	−1.0	−1.2
2P1/2–10D3/2	789145915	0.05	−1.0	−0.6
2P1/2–11S1/2	794852408.8	1.2	−0.5	0.6
2P1/2–11D3/2	794852467.8	0.7	−1.0	−0.2
2P1/2–12S1/2	799192722.9	1.2	−0.5	0.8
2P1/2–12D3/2	799192768.321	0.013	−1.0	0.1
2S1/2–2P3/2	9911.202	0.012	0.8	2.1
2S1/2–3P1/2	456681549.96	0.21	−1.4	−5.0
2S1/2–3S1/2	456681864.78	0.22	−0.4	−4.3
2S1/2–3P3/2	456684800.05	0.21	−1.5	−5.1
2S1/2–4P1/2	616520017.569	0.015	−0.3	−2.9
2S1/2–4S1/2	616520150.636	0.01	0.4	−2.4
2S1/2–4P3/2	616521388.671	0.01	−0.3	−3.0
2S1/2–4D5/2	616521843.443	0.024	1.3	−9.6
2S1/2–5P1/2	690502203.4	1.1	0.1	−1.2
2S1/2–5S1/2	690502271.6	1.1	0.5	−0.9
2S1/2–5P3/2	690502905.4	1.1	0.1	−1.3
2S1/2–6P1/2	730689977.6	0.03	−0.1	−0.3
2S1/2–6S1/2	730690017.097	0.021	0.2	−0.1
2S1/2–6P3/2	730690383.86	0.04	−0.1	−0.3
2S1/2–6D5/2	730690518.592	0.011	0.4	−2.3
2S1/2–7P1/2	754921901.3	1.2	−0.1	0.5
2S1/2–7S1/2	754921926.2	1.2	0.1	0.7
2S1/2–7P3/2	754922157.2	1.2	0.0	0.6
2S1/2–8P1/2	770649333.338	0.018	0.1	1.4
2S1/2–8S1/2	770649350.012	0.009	0.3	1.5
2S1/2–8D3/2	770649504.45	0.08	0.0	0.4
2S1/2–8P3/2	770649504.729	0.019	0.1	1.4
2S1/2–8D5/2	770649561.584	0.007	0.3	0.5
2S1/2–9P1/2	781431998.7	1.2	0.3	2.0
2S1/2–9S1/2	781432010.4	1.2	0.4	2.0

Table 4: (continued)

interval	ΔE_{Ritz} (MHz) (Ritz values)	Unc. (MHz)	$\Delta E_{Ritz} - \Delta E_{calc}$ (MHz) α_{geom}	α_{Codata}
2S1/2–9P3/2	781432119.1	1.2	0.3	2.0
2S1/2–10P1/2	789144769.9	1.2	0.5	2.5
2S1/2–10S1/2	789144778.4	1.2	0.5	2.5
2S1/2–10P3/2	789144857.6	1.2	0.4	2.5
2S1/2–10D5/2	789144886.41	0.4	0.2	1.7
2S1/2–11P1/2	794851344.5	1.2	0.4	2.8
2S1/2–11S1/2	794851350.9	1.2	0.5	2.8
2S1/2–11P3/2	794851410.4	1.2	0.4	2.8
2S1/2–12P1/2	799191660.1	1.2	0.4	3.0
2S1/2–12S1/2	799191665	1.2	0.4	3.0
2S1/2–12D3/2	799191710.473	0.01	0.1	2.4
2S1/2–12P3/2	799191710.9	1.2	0.4	3.0
2S1/2–12D5/2	799191727.404	0.007	0.2	2.4
2P3/2–3S1/2	456671953.58	0.22	−1.1	−6.4
2P3/2–3D3/2	456674883.5	0.6	−4.9	−25.3
2P3/2–3D5/2	456675966.74	0.22	1.4	−22.9
2P3/2–4S1/2	616510239.434	0.016	−0.4	−4.5
2P3/2–4D3/2	616511475.45	0.23	−2.0	−12.5
2P3/2–4D5/2	616511932.24	0.03	0.5	−11.7
2P3/2–5S1/2	690492360.4	1.1	−0.3	−2.9
2P3/2–5D3/2	690492991.4	0.7	−2.9	−8.9
2P3/2–5D5/2	690493225.3	0.7	−1.7	−8.4
2P3/2–6S1/2	730680105.895	0.024	−0.6	−2.2
2P3/2–6D3/2	730680472	0.04	−1.2	−4.7
2P3/2–6D5/2	730680607.39	0.016	−0.4	−4.4
2P3/2–7S1/2	754912015	1.2	−0.7	−1.4
2P3/2–7D3/2	754912245.7	0.7	−0.9	−2.8
2P3/2–7D5/2	754912331	0.7	−0.4	−2.6
2P3/2–8S1/2	770639438.81	0.015	−0.5	−0.6
2P3/2–8D3/2	770639593.248	0.015	−0.8	−1.7
2P3/2–8D5/2	770639650.382	0.014	−0.5	−1.5
2P3/2–9S1/2	781422099.2	1.2	−0.4	0.0
2P3/2–9D3/2	781422207.5	0.7	−0.8	−0.9
2P3/2–9D5/2	781422247.6	0.7	−0.6	−0.9
2P3/2–10S1/2	789134867.2	1.2	−0.3	0.5
2P3/2–10D3/2	789134945.95	0.05	−0.8	−0.4
2P3/2–10D5/2	789134975.21	0.04	−0.6	−0.3
2P3/2–11S1/2	794841439.7	1.2	−0.3	0.8
2P3/2–11D3/2	794841498.7	0.7	−0.8	−0.1
2P3/2–11D5/2	794841520.7	0.7	−0.7	0.0
2P3/2–12S1/2	799181753.8	1.2	−0.4	0.9
2P3/2–12D3/2	799181799.271	0.015	−0.7	0.3
2P3/2–12D5/2	799181816.202	0.014	−0.6	0.4

Table 4: (continued)

interval	ΔE_{Ritz} (MHz) (Ritz values)	Unc. (MHz)	$\Delta E_{Ritz} - \Delta E_{calc}$ (MHz) α_{geom}	α_{Codata}
3P1/2–3S1/2	314.82	0.05	1.1	0.7
3P1/2–3D3/2	3244.8	0.6	−2.6	−18.2
3P1/2–3P3/2	3250.09	0.03	−0.1	0.0
3S1/2–3D3/2	2929.9	0.6	−3.8	−18.9
3S1/2–3P3/2	2935.27	0.06	−1.2	−0.8
3S1/2–3D5/2	4013.16	0.05	2.6	−16.5
3D3/2–3P3/2	5.3	0.6	2.5	18.1
3D3/2–3D5/2	1083.2	0.6	6.3	2.4
3P3/2–3D5/2	1077.89	0.07	3.7	−15.8
4P1/2–4S1/2	133.067	0.018	0.7	0.6
4P1/2–4P3/2	1371.102	0.018	−0.1	0.0
4P1/2–4D3/2	1369.08	0.23	−0.9	−7.5
4S1/2–4D3/2	1236.02	0.23	−1.6	−8.0
4P3/2–4D5/2	454.77	0.03	1.6	−6.6
5P1/2–5S1/2	68.201	0.019	0.4	0.4
5P1/2–5D3/2	699.2	1.3	−2.2	−5.6
5P1/2–5P3/2	702.019	0.012	0.0	0.0
5S1/2–5P3/2	633.818	0.022	−0.4	−0.4
5D3/2–5D5/2	233.92	0.08	1.3	0.5
5P3/2–5D5/2	231.1	1.3	−0.9	−5.1
8D3/2–8D5/2	57.134	0.01	0.3	0.1
12D3/2–12D5/2	16.931	0.012	0.1	0.1

Notes:

a) Ritz series limit [Kramida 2010, Table D].
b) NIST: Atomic Spectra Database 78 [version 5.11]: Ionization Energies Form. Energy has been determined from bound-state QED ab initio calculations.

Table 5: Frequencies of fine-structure transitions in *deuterium* derived from the level-optimization procedure [Kramida 2010, Table 7].

interval	ΔE_{Ritz} (MHz) (Ritz values)	Unc. (MHz)	$\Delta E_{Ritz} - \Delta E_{calc}$ (MHz) α_{geom}	α_{Codata}
Ionization [a]	**3288981521.1**	**2.3**	**−1.1**	**3.1**
Ionization [b]	3288981522.062	0.003	−0.09	4.1
1S1/2–2P1/2	2466731348.24	0.06	0.7	2.5
1S1/2–2S1/2	2466732407.52171	0.00015	0.1	0.5
1S1/2–2P3/2	2466742320.1	0.3	0.0	2.0
1S1/2–3P1/2	2923538219.2	0.3	−0.6	−3.9
1S1/2–3S1/2	2923538534.6	0.5	0.7	−3.0
1S1/2–3P3/2	2923541470.1	0.3	−0.9	−4.1
1S1/2–4P1/2	3083420177.53	0.17	−0.6	−3.0
1S1/2–4S1/2	3083420311.095	0.02	0.5	−2.1
1S1/2–4P3/2	3083421549.28	0.15	−0.4	−2.8
1S1/2–5P1/2	3157422491	7	−3.0	−4.1
1S1/2–5S1/2	3157422559	6	−2.9	−4.0
1S1/2–5P3/2	3157423193	7	−3.3	−4.3
1S1/2–5D5/2	3157423433.2	2.3	5.0	−0.3
1S1/2–6P1/2	3197621201	7	−2.5	−2.5
1S1/2–6S1/2	3197621241	6	−1.8	−1.8
1S1/2–6P3/2	3197621608	7	−1.9	−1.9
1S1/2–6D5/2	3197621746.3	2.3	2.2	−0.2
1S1/2–7P1/2	3221859720	6	−0.7	0.1
1S1/2–7S1/2	3221859745	6	−0.4	0.4
1S1/2–7P3/2	3221859976	6	−0.6	0.2
1S1/2–7D5/2	3221860061.9	2.3	0.8	0.1
1S1/2–8P1/2	3237591432.01	0.3	0.1	1.5
1S1/2–8S1/2	3237591448.768	0.07	0.3	1.7
1S1/2–8P3/2	3237591603.48	0.04	0.1	1.6
1S1/2–9P1/2	3248377032	7	0.9	2.8
1S1/2–9S1/2	3248377044	6	1.2	3.1
1S1/2–9P3/2	3248377153	7	1.5	3.4
1S1/2–9D5/2	3248377191.5	2.3	0.2	1.4
1S1/2–10P1/2	3256091901	7	0.2	2.5
1S1/2–10S1/2	3256091910	6	0.7	3.0
1S1/2–10P3/2	3256091989	7	0.4	2.7
1S1/2–11P1/2	3261800029	7	0.8	3.4
S1/2–11S1/2	3261800035	6	0.5	3.0
1S1/2–11P3/2	3261800095	7	0.9	3.5
1S1/2–11D5/2	3261800116.1	2.3	0.2	2.4
1S1/2–12P1/2	3266141526	6	1.2	4.0
1S1/2–12S1/2	3266141531	6	1.3	4.1
1S1/2–12P3/2	3266141577	7	1.4	4.2
2P1/2–2S1/2	1059.28	0.06	−0.7	−1.9

Table 5: (continued)

interval	ΔE_{Ritz} (MHz) (Ritz values)	Unc. (MHz)	$\Delta E_{Ritz} - \Delta E_{calc}$ (MHz) α_{geom}	α_{Codata}
2P1/2–2P3/2	10971.9	0.4	−0.7	−0.4
2P1/2–3S1/2	456807186.4	0.5	0.0	−5.4
2P1/2–3D3/2	456810114.2	1.8	−5.6	−26.3
2P1/2–4S1/2	616688962.86	0.07	−0.2	−4.5
2P1/2–4D3/2	616690198.83	0.24	−1.8	−12.5
2P1/2–5S1/2	690691211	7	−3.3	−6.3
2P1/2–5D3/2	690691850.8	2.3	2.8	−3.4
2P1/2–6D3/2	730890262.7	2.3	0.8	−2.9
2P1/2–7S1/2	755128397	7	−0.9	−1.9
2P1/2–7D3/2	755128628.2	2.3	−0.6	−2.8
2P1/2–8S1/2	770860100.53	0.6	−0.5	−0.8
2P1/2–8D3/2	770860254.98	0.06	−0.7	−1.8
2P1/2–9S1/2	781645696	7	0.8	0.9
2P1/2–9D3/2	781645803.1	2.3	−0.8	−1.2
2P1/2–10S1/2	789360562	7	0.3	0.8
2P1/2–10D3/2	789360640.26	0.07	−0.7	−0.6
2P1/2–11S1/2	795068687	7	0.0	0.8
2P1/2–11D3/2	795068745.9	2.3	−0.6	−0.1
2P1/2–12S1/2	799410183	7	0.8	1.9
2P1/2–12D3/2	799410227.32	0.06	−0.7	0.1
2S1/2–2P3/2	9912.6	0.3	−0.1	1.5
2S1/2–3P1/2	456805811.7	0.3	−0.7	−4.4
2S1/2–3S1/2	456806127.1	0.5	0.7	−3.5
2S1/2–3P3/2	456809062.6	0.3	−0.9	−4.6
2S1/2–4P1/2	616687770.01	0.17	−0.6	−3.5
2S1/2–4S1/2	616687903.573	0.02	0.5	−2.6
2S1/2–4P3/2	616689141.76	0.16	−0.4	−3.3
2S1/2–4D5/2	616689596.72	0.04	1.6	−9.5
2S1/2–5P1/2	690690083	6	−3.6	−5.1
2S1/2–5P3/2	690690785	7	−3.8	−5.4
2S1/2–6P1/2	730888794	7	−2.0	−2.5
2S1/2–6P3/2	730889200	7	−2.4	−2.9
2S1/2–7P1/2	755127312	7	−1.2	−0.9
2S1/2–7P3/2	755127568	7	−1.2	−0.8
2S1/2–8P1/2	770859024.49	0.03	0.0	1.0
2S1/2–8P3/2	770859195.96	0.04	0.0	1.0
2S1/2–9P1/2	781644625	7	1.3	2.8
2S1/2–9P3/2	781644745	7	0.9	2.4
2S1/2–10P1/2	789359494	7	0.7	2.5
2S1/2–10P3/2	789359582	7	0.9	2.7
2S1/2–11P1/2	795067621	6	0.3	2.4
2S1/2–11P3/2	795067687	6	0.3	2.4
2S1/2–12P1/2	799409119	7	1.7	4.0

Table 5: (continued)

interval	ΔE_{Ritz} (MHz) (Ritz values)	Unc. (MHz)	$\Delta E_{Ritz} - \Delta E_{calc}$ (MHz) α_{geom}	α_{Codata}
2S1/2–12P3/2	799409169	7	0.9	3.2
2P3/2–3S1/2	456796214.5	0.6	0.7	−5.0
2P3/2–3D3/2	456799142.3	1.8	−4.9	−25.8
2P3/2–4S1/2	616677991	0.3	0.5	−4.1
2P3/2–4D3/2	616679227	0.4	−1.0	−12.0
2P3/2–4D5/2	616679684.1	0.3	1.7	−11.0
2P3/2–5S1/2	690680239	7	−2.7	−5.9
2P3/2–5D3/2	690680878.9	2.3	3.6	−2.9
2P3/2–5D5/2	690681113	2.3	5.0	−2.4
2P3/2–6S1/2	730878921	7	−1.6	−3.7
2P3/2–6D3/2	730879290.9	2.3	1.6	−2.4
2P3/2–6D5/2	730879426.3	2.3	2.3	−2.1
2P3/2–7S1/2	755117425	7	−0.3	−1.5
2P3/2–7D3/2	755117656.4	2.3	0.2	−2.2
2P3/2–7D5/2	755117741.7	2.3	0.7	−2.0
2P3/2–8S1/2	770849128.7	0.3	0.3	−0.3
2P3/2–8D3/2	770849283.1	0.3	0.0	−1.4
2P3/2–8D5/2	770849340.3	0.3	0.4	−1.2
2P3/2–9S1/2	781634724	7	1.4	1.2
2P3/2–9D3/2	781634831.3	2.4	0.0	−0.7
2P3/2–9D5/2	781634871.4	2.3	0.2	−0.6
2P3/2–10S1/2	789349590	7	0.9	1.1
2P3/2–10D3/2	789349668.4	0.3	0.1	−0.1
2P3/2–10D5/2	789349697.7	0.3	0.3	0.0
2P3/2–11S1/2	795057715	7	0.6	1.1
2P3/2–11D3/2	795057774	2.3	0.1	0.3
2P3/2–11D5/2	795057796	2.3	0.2	0.4
2P3/2–12S1/2	799399211	7	1.4	2.2
2P3/2–12D3/2	799399255.5	0.3	0.1	0.6
2P3/2–12D5/2	799399272.4	0.3	0.2	0.6
3P1/2–3S1/2	315.4	0.4	1.3	1.0
3P1/2–3P3/2	3250.9	0.4	−0.3	−0.2
3D3/2–3D5/2	1083.6	2.4	6.4	2.5
4P1/2–4S1/2	133.57	0.17	1.1	0.9

Notes:

a) Ritz series limit [Kramida 2010, Table H].
b) NIST: Atomic Spectra Database 78 [version 5.11]: Ionization Energies Form. Energy has been determined from bound-state QED ab initio calculations.

Table 9: Absolute values of the hyperfine splitting frequencies in H and D calculated by scaling from the hfs of 1S1/2.

			hydrogen		*deuterium*	
$(\Delta E)_{hfs}$	$1S1/2$	(MHz)	1420.405 751 768(1)	a)	327.384 352 5222(17)	a)
$\tilde{B}$		(ppm)	0.080 997 276	b)	0.024 884 934	b)
$(\Delta E)_{hfs}$	$2S1/2$	(MHz)	**177.55 15**		**40.92 32**	
			177.55 69	a)	**40.92 45**	a)
	$3S1/2$		52.60 77		12.12 54	
	$4S1/2$		22.19 38		5.11 54	
	$5S1/2$		11.36 32		2.61 91	
	$6S1/2$		6.57 59		1.51 57	
	$7S1/2$		4.14 11		0.95 45	
	$8S1/2$		2.77 42		0.63 94	
	$9S1/2$		1.94 84		0.44 91	
	$10S1/2$		1.42 04		0.32 74	
	$11S1/2$		1.06 72		0.24 60	
	$12S1/2$	(MHz)	0.82 20		0.18 95	
	$2P1/2(F=1)$	(MHz)	**59.18 39**			
	$2P3/2(F=2)$		23.67 33			
	$3P1/2(F=1)$		17.53 59			
	$3P3/2(F=2)$		7.01 43			
	$3D3/2(F=2)$		4.20 86			
	$3D5/2(F=3)$		2.70 55			
	$4D5/2(F=3)$		1.14 14			
	$4F7/2(F=4)$		0.60 39			
	$7F5/2(F=3)$		0.15 21			
	$8D3/2(F=2)$		0.22 19			
	$8D5/2(F=3)$		0.14 27			
	$8F5/2(F=3)$	(MHz)	0.10 19			
	$4D5/2(F=7/2)$	(MHz)			0.20 46	
	$4D5/2(F=5/2)$				0.14 62	
	$8D5/2(F=7/2)$				0.02 56	
	$8D5/2(F=5/2)$	(MHz)			0.01 83	

Notes:

Hfs values without a reference are derived using formula (8) and may be compared against the theoretical values presented by Kramida in 2010 [Hydrogen: Table A and Table 1; deuterium: Table B and Table 2].

a) Experimental value [Kramida 2010, p. 591].
b) Calculated from the 1S hfs using formula (6).